TEKNILLINEN TIEDEKUNTA

MECHANICAL PROPERTIES AND DRYING SHRINKAGE OF FIBRE REINFORCED ALKALI ACTIVATED FLY ASH/SLAG BINDERS USING CERAMIC WASTE AGGREGATE

Mikko Naalisvaara

PROCESS ENGINEERING

Bachelor's Thesis

May 2018

TEKNILLINEN TIEDEKUNTA

MECHANICAL PROPERTIES AND DRYING SHRINKAGE OF FIBRE-REINFORCED ALKALI ACTIVATED FLY ASH/SLAG BINDERS USING CERAMIC WASTE AGGREGATE

Mikko Naalisvaara

Thesis Supervisor: Zahra Abdollahnejad, PhD

PROCESS ENGINEERING

Bachelor's Thesis

May 2018

TIIVISTELMÄ
OPINNÄYTETYÖSTÄ Oulun yliopisto Teknillinen tiedekunta

Koulutusohjelma (kandidaatintyö, diplomityö) Prosessitekniikka	Pääaineopintojen ala (lisensiaatintyö)
Tekijä Naalisvaara, Mikko	Työn ohjaaja yliopistolla Abdollahnejad, Zahra. PhD

Työn nimi

Kuiduilla vahvistettujen alkali-aktivoitujen lentotuhka- ja masuunikuonasideaineiden mekaaniset ominaisuudet ja kutistuminen keraamista jätettä rakenneaineena käytettäessä

Opintosuunta	Työn laji	Aika	Sivumäärä
Kuitu- ja partikkelitekniikka	Kandidaatintyö	Toukokuu 2018	38

Tiivistelmä

Portlandsementti, eräs yleisimmistä rakennusmateriaaleista, on merkittävä kasvihuonekaasupäästöjen aiheuttaja. Portlandsementin valmistusprosessi käyttää paljon energiaa, ja se kuluttaa maapallon luonnonvaroja hälyttävällä tahdilla. Uusia materiaaleja, joilla Portlandsementti voitaisiin korvata, ollaan tutkittu ja kehitelty jo vuosikymmeniä, ja eräs lupaavista ehdokkaista on alkali-aktivoidut materiaalit. Näiden valmistaminen ei vaadi paljoa luonnonvaroja, sillä useita teollisuuden sivutuotteita voidaan hyödyntää lähes suoraan raaka-aineina, kuten masuunikuonaa ja lentotuhkaa. Lisäksi alkali-aktivaatioreaktio on huomattavasti Portlandsementin valmistuksessa tarvittavia kemiallisia reaktioita ympäristöystävällisempi. Yksi-osaiset alkali-aktivoidut sideaineet ovat kiinteässä muodossa veden lisäämiseen asti, joten niitä on helppoa ja turvallista käsitellä ja kuljettaa. Tässä työssä suoritettiin kokeita, joiden avulla mitattiin erään alkali-aktivoiduista sideaineista valmistetun betonin mekaanisia ominaisuuksia, sekä kuivumisen aiheuttamaa kutistumista. Kokeissa tutkittiin optimaalista lentotuhkan ja masuunikuonan välistä suhdetta, sekä kolmen erilaisen kuidun vaikutusta lisäaineena. Rakenneaineena käytettiin keraamista jätettä, eli posliinia, joka murskattiin haluttuun raekokoon leukamyllyllä. Jätteenä posliini on huono kierrätettävä, joten sille mahdollisten käyttötarkoituksien löytäminen on tärkeää.

Tulosten perusteella betonin pohjaksi valittiin lentotuhka-masuunikuonasuhteeltaan 40/50 koostuva variantti. Polypropyleeni- (PP), basaltti- (Ba) ja polyvinyylialkoholikuituja (PVA) testattiin eri suhteissa niin, että niiden kokonaisosuus aineen tilavuudesta oli 1,5 %. Tulosten mukaan yleisesti kuitujen lisääminen lisäsi näytteiden taivutuslujuutta. Jäätymis-sulamissyklit heikensivät kuidullisia näytteitä enemmän kuin kuiduttomia taivutuslujuustestissä, mutta puristuslujuudessa vaikutusta ei juurikaan havaittu. Kuivumisen aiheuttama kutistuminen vaihteli eri kuituyhdistelmien välillä, mutta yleisesti ottaen kuituyhdistelmät yksittäisten kuitujen sijaan aiheuttivat vähiten kutistumista.

Muita tietoja

ABSTRACT
FOR THESIS

University of Oulu Faculty of Technology

Degree Programme (Bachelor's Thesis, Master's Thesis)	Major Subject (Licentiate Thesis)
Process Engineering	
Author	**Thesis Supervisor**
Naalisvaara, Mikko	Abdollahnejad, Zahra. PhD

Title of Thesis

Mechanical properties and drying shrinkage of fibre-reinforced alkali activated fly ash/slag binders using ceramic waste aggregate

Major Subject	Type of Thesis	Submission Date	Number of Pages
Fibre and Particle technology	Bachelor's Thesis	May 2018	38

Abstract

Ordinary Portland Cement (OPC), one of the most used construction materials, is a significant contributor to greenhouse gas emissions, such as carbon dioxide. The manufacturing process of OPC requires large amounts of energy and it consumes Earth's natural resources at a high rate. New methods to replace OPC have been developed for a few decades now, and one of the promising method is a class of materials known as alkali-activated materials (AAM). AAM's require less raw resources to manufacture, due to utilizing various industrial by-products, such as blast furnace slag and fly ash. One-part alkali-activated binders require only dry materials that can be mixed and water is being added to the binder as the last step. This makes them easy to handle and transport. In this thesis, experiments regarding the mechanical properties and drying shrinkage were conducted on a set of different samples, including different fly ash-slag mix compositions and fibre combinations. Crushed ceramic waste was used as an aggregate, because it is currently a form of waste with very little use. It was found that using 40 % slag and 50 % fly ash was a desirable mix composition, and so it acted as the reference for fibre-reinforced mix compositions. Polypropylene (PP), basalt (Ba) and polyvinyl alcohol fibres (PVA) were tested in different combinations, with the total amount of fibres in each specimen at 1,5% (total volume). Results showed that generally the addition of fibres increased the total flexural strength. Freeze-thaw test results showed that flexural strength loss was lower with fibre-reinforced samples, and compressive strength generally isn't negatively affected. Hybrid fibre mixtures showed the most promising results in terms of reducing drying shrinkage rate.

Additional Information

TABLE OF CONTENTS

LIST OF SYMBOLS AND ABBREVIATIONS

AAM	Alkali-activated material
OPC	Ordinary Portland Cement
PVA	Polyvinyl alcohol
PP	Polypropylene
AASB	Alkali-activated slag-based binder
GGBFS	Ground-granulated blast furnace slag

–	——

d	Particle size
σ_c	Compressive strength
σ_f	Flexural strength
ρ	Density
L	Span length
F	Force

1 INTRODUCTION

Concrete is a widely used construction material, which traditionally has relied on Portland Cement as a binder along with aggregate and water. The production of Ordinary Portland Cement (OPC) has significant carbon dioxide emissions, which are approximately 8 % of the total global human-caused CO_2 emissions (Davidovits, 1994).

In the OPC manufacturing process, the decarbonation reaction of limestone at extreme temperatures (1400 – 1500 °C) is the major cause (50 – 60 %) of the CO_2 emissions (Luukkonen et al., 2018).

It has been shown by Unal and Lavat et al. that ceramic waste can substitute up to 40 % by weight of OPC and according to European standard EN 206-1, up to 35 % by weight of concrete can be replaced with ceramic waste (Amin et al., 2016).

The purpose of this thesis is to investigate the potential of using ceramic waste as an aggregate in alkali-activated binders.

1.1 Alkali-activated binders

An alkali-activated binder is composed a solid aluminosilicate precursor (fly ash, slag, metakaolin, silica fume), which is activated by an alkali solution. In general, the alkali solution is prepared by combination of sodium hydroxide and sodium silicate or combination of solid activator and water. The process is called alkali-activation (Gao, 2017)

In Figure 1, an illustration is depicted common classification of binders are used. In this figure, common binders are placed on a three-dimensional coordinate system, where each axis demonstrates the chemical contents of different raw materials. As seen, alkali-activated materials occupy a large volume within the system, indicating a wide range of possibilities.

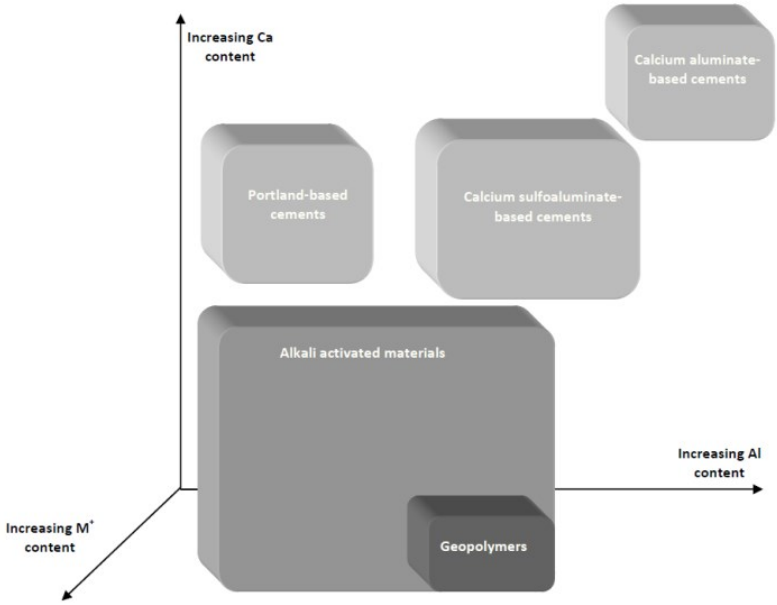

Figure 1: Classification of common binders. (Provis et al., 2014)

There are two main types of alkali-activated binders. The more common and traditional way is two-part alkali activated binders. A two-part alkali-activated binder includes alkali solutions, which are chemicals with harsh properties like corrosiveness, hard to handle on site, high viscosity and not user-friendly (Abdollahnejad et al., 2018).

The second type of alkali-activated binder is a one-part alkali activated binder, which requires only water to be added to the mixture and alkali activator as solid component. There are many different advantages in one-part alkali activated binder in comparison to the traditional two-part alkali activated binder, such as being easy and safe. This makes one-part alkali activated binders good option for on-site casting, which make them a good option for commercial use in construction applications. (Abdollahnejad et al., 2018)

The reaction mechanism of alkali-activated materials differs from OPC concrete. Alkali-activated binders with a high calcium content activated in a moderately alkaline environment. The main product of the reaction is a calcium aluminium silicate hydrate gel, which forms a dense matrix with decent mechanical properties. (Gao, 2017)

1.1.1 Alkali-activated slag-based binders

Blast furnace slag is the waste product of metallurgical smelting process. In extremely hot temperatures, the metal separates from the rest of the ore, leaving behind oxidised, silicate-rich slag. When the slag is cooled down rapidly from its initial state, granulation takes place along with other chemical reactions, giving slag its cementitious nature. (Seymour, 2010).

Ground-granulated blast furnace slag (GGBFS) can be used in one-part alkali activated binders as a calcium-rich aluminosilicate precursor. The compressive strength of alkali-activated slag binders is high at the early ages and initial and final setting time are very fast. (Abdollahnejad et al., 2018).

GGBFS-binders have some draw backs such as high rate of drying shrinkage. The shrinkage leads to the formation of cracks in the mixture surface, which has a negative impact on durability and mechanical properties. (Abdollahnejad et al., 2018).

1.1.2 Alkali-activated fly ash-based binders

Fly ash can be used as an ingredient in one-part alkali-activated binders. Industrial fly ash needs an alkali activator to be used as a binder (Fernández-Jiménez, 2005). Fly ash can be considered as the main source of silica and alumina in geopolymer concretes. (Pilehvar et al., 2018).

The reaction product of two-part alkali-activated fly ash is an alkaline silicoaluminate gel. OH^- ion acts as a catalyst and Na^+ ion as the structure-forming agent in the alkali-activation reaction. Silicon and Aluminium form in a random distribution in a tetrahedral geometry in polymeric chains, after the activation. (Fernández-Jiménez, 2005).

1.1.3 Fibre reinforced alkali-activated materials

According to previous studies on alkali activated slag binders, one of the main drawbacks of using slag in alkali-activated binders is their high shrinkage rate. According to a study conducted by J. Zhu et al., adding polypropylene (PP) fibre to the alkali-activated slag-based material increased the tensile and compressive strengths. (Zhu et al., 2018).

In the case of GGBFS, adding fibre to the matrix reduces the rate of shrinkage. As discussed previously, the high rate of shrinkage leads to cracks formation. (Abdollahnejad et al., 2018).

To minimise the shrinkage, various methods can be combined to achieve optimal results. In this thesis, a combination of GGBFS and fly ash is used as the alkali-activated binder, and fibres are added in the mixture mainly to control the drying shrinkage.

1.2 Slag

Slag is an industrial by-product that is produced for instance in the production of pig iron from iron ore. It is produced by rapidly cooling molten blast furnce slag with water. (Seymour, 2010).

According to Seymour (2010), GGBFS has the similar chemical constituents as OPC, but in different ratios.

During the production of OPC, one tonne of CO_2 is produced per a tonne of OPC. In addition, two kilograms of SO_2, 3.5 kilograms of NO_x and two kilograms of CO is produced per a tonne of OPC. On the contrary, during the production of GGBFS, a minimal amount of CO_2 is produced, and a zero amount of toxic gases (SO_2, NO_x and CO) are produced. (Seymour, 2010).

1.3 Fly ash

Fly ash is a by-product of power plants that burn coal as their fuel. Fine particles of coal ignite in the furnace, where temperatures exceed 1200 °C. The mineral residue left behind contains iron oxides and aluminosilicates, which after cooling, form amorphous, spherical and hollow particles. Fly ash can also contain crystalline phases of minerals like magnetite and quartz, which form from the raw materials at the extreme temperatures. The exact chemical composition of fly ash depends on variables like the temperature of the boiler in which the coal is burned (Sankar et al., 2017).

1.4 Sodium metasilicate

Sodium metasilicate can be produced by two methods: furnace process and hydrothermal process. The furnace process uses ordinary sand and soda ash as raw materials. They are heated in a furnace, where after milling and agglomeration of sodium silicate, anhydrous sodium metasilicate is formed. The hydrothermal process produces hydrous metasilicate (Davidovits, 2008).

1.5 Ceramic wastes

In this study, crushed ceramic waste from sanitary equipment is used as an aggregate. The ceramic is crushed using a jaw-mill, and the crushed material is sieved using 4 mm and 0.5 mm diameter sizes. The crushed material left in between of the sieves (4 mm > d > 0.5 mm, where d is the particle size) is used as the aggregate.

Crushed ceramic waste has previously shown promising results as a replacement for traditional river sand used as a concrete aggregate. In 2015 Ariffin et al., reported that using ceramic waste aggregate in a geopolymer concrete showed an improvement in compressive strength, flexural strength and splitting tensile strength. These results present evidence for ceramic waste aggregate as a useful component to be considered in designing a high strength geopolymer concrete (Ariffin et al., 2015).

Waste ceramic is a suitable aggregate for an alkali-activated one-part binder because it can provide reactive silica, which is an essential component in the alkali-activation reaction that makes the gel formation. In addition, using ceramic waste as the silica source has some ecological advantages, like conserving energy and natural resources, as well as reducing the carbon footprint of the product and the cost (Pacheco-Torgal et al., 2010).

One study showed that crushed ceramic waste aggregate in a traditional OPC based concrete can be used. The study showed that the strength of the samples was high and the crushing ratio was low. The water absorption and the abrasion resistance of the samples was also measured to be high compared to control samples. Because of the high strength parameters, the samples performed better in high temperatures as well (Halicka et al., 2013).

1.6 Fibres

1.6.1 Polyvinyl Alcohol Fibre

Polyvinyl alcohol (PVA) fibre has good physical properties for reinforcing concrete. It has relatively high elastic modulus, durability and tensile strength, and is therefore a suitable fibre option, as pointed out by Manafaluthy et al. (2017).

The results reported in the study of Manafaluthy et al. (2017) were the following: 0.8 % PVA fibre reinforced specimens had the highest strength. The compressive strength increased by 9.95 %, splitting strength by 61.69 % and direct tensile strength increased by 32.78 %. Compressive strength did not see a meaningful change, because the properties of PVA mainly resist under tensile and flexural load. In addition, Manafaluthy et al. (2017) recommends adding 0.5 % PVA to geopolymer concrete to improve the mechanical properties. 0.8 % may lead to higher mechanical properties, but the workability is decreased.

The results of the study show promising potential for using PVA fibre in geopolymers especially in improvement of tensile and flexural strength.

1.6.2 Basalt

Basalt is the most common rock found on earth and the fibres are manufactured by melting basalt rock, and there are two methods to produce the fibrous product: the Junkers and the Spinneret method. The density of basalt allows it not to float or sink in wet concrete; it will stay at its place after mixing. Basalt, like other fibres, does not affect concrete's compressive strength, only its tensile strength and toughness (Kiisa et al., 2016).

1.6.3 Polypropylene Fibre

Polypropylene (PP) fibre is a synthetic substance. PP fibre was tested as reinforcement in an alkali-activated slag based cementitious material, where it performed better than the control sample and a sample with plant fibre reinforcement (Zhu et al., 2018). PP fibres become tightly coupled within the matrix, leading to higher stress resistance. PP fibre was recorded to withstand significantly more tensile stress. The peak of non-reinforced AASCM, according to study by Zhu et al. (2018), was recorded at $\varepsilon \approx 0.95$ % and $\sigma \approx 1.05$ MPa, while the PP fibre reinforced sample was recorded at $\varepsilon \approx 2.50$ % and $\sigma \approx 3.40$ MPa. Similar results were achieved in compressive tests, where PP fibre outnumbered non-reinforced sample with nearly twice as much pressure in MPa (Zhu et al., 2018).

1.6.4 Fibre specifications

The fibres used in this thesis are listed in Table 1 with their relevant technical specifications. The values were provided by the manufacturers of the fibres.

Table 1: Physical properties of the fibres

Fibre	Diameter (μm)	Cut length (mm)	Tensile strength (MPa)	Density (kg/m^2)
PVA	40-200	8-18	1000-1600	1.30
PP	22.3	12	220-340	0.91
Basalt	18	25	4100-4840	2.80

2 MATERIALS AND METHOD

Five different mix compositions are prepared and tested, including the reference sample. The mix compositions are listed in Table 2.

Table 2: Mix compositions (first phase)

Mixtures	Slag (%)	Fly ash (%)	Sodium Silicate (%)	Water/binder (%)	Porcelain ceramic/binder
Reference	90	0	10	35	2
F1CW	80	10	10	35	2
F2CW	60	30	10	35	2
F3CW	40	50	10	35	2
F4CW	20	80	10	35	2

The sample preparation and test procedure are as follows:

The dry components (slag, fly ash, ceramic waste and anhydrous sodium metasilicate) are mixed in a Kenwood industrial mixer for two minutes with minimum speed. Normal tap water is weighed on the digital scale and added to the mix gradually and mixed for 3 more minutes to ensure homogeneity.

The mixture is poured into standard prismatic moulds (40 x 40 x 160 mm). The mould is filled in two steps. First, the moulds are filled up to half and the shaker is used for 60 times at a frequency of 1 impact per second. Then the moulds are filled to the top and the shaker is used the same as the previous step.

The samples are labelled and put into a controlled environment that has its humidity and temperature monitored, for 24 hours. The temperature is controlled at 23 °C and relative humidity at 35 %. The specimens were demoulded and stored in the controlled environment until the test date.

The samples are tested after 7 and 28 days for flexural and compressive strength.
In the next phase, F3CW was chosen to be used as reference. The technical properties of F3CW can be improved by incorporating fibres.
In this thesis, the effects of different fibres on reducing the drying shrinkage of the reference mix composition (F3CW) which was selected from the first phase will be evaluated. The designed mix compositions are listed in Table 3.

Table 3: Mix compositions (second phase)

Mixture	Fibres (%)/total volume
Mix 1	PVA 1.5
Mix 2	PP 1.5
Mix 3	Basalt 1.5
Mix 4	PVA 0.75 + PP 0.75
Mix 5	PVA 0.75 + Basalt 0.75
Mix 6	Basalt 0.75 + PP 0.75
Mix 7	PVA 0.5 + PP 1.0
Mix 8	Basalt 0.5 + PP 1.0
Mix 9	Basalt 1 + PP 0.5
Mix 10	PVA 1.0 + Basalt 0.5
Mix 11	PVA 0.5 + Basalt 1.0
Mix 12	PVA 1.0 + PP 0.5

The fibre reinforced specimens are prepared in a same way as the non-reinforced ones. The fibres are weighed and added after the water has been poured and mixed for one minute. The fibres are added gradually, to prevent the formation of clumps.

2.1 Compressive strength

The compressive strength test measures the samples strength under a compressive load. The load measured by the instrument is as shown in Equation 1.

$$\sigma_c = \frac{F}{A} \tag{1}$$

Where σ_c is the compressive strength in MPa, F is the compressive load in kN, and A is the surface area of the sample on which the load is asserted, in mm^2.

2.2 Flexural strength

The flexure of the samples was measured using the Three Point Bending (TPB) test.

Equation 2 is used to calculate the flexural strength of the sample:

$$\sigma_f = \frac{3FL}{2bh^2} \tag{2}$$

Where σ_f is the flexural strength, F is the total flexural load, L is the testing span (100 mm), and b and h are the cross-sectional dimensions of the sample (both are 40 mm).

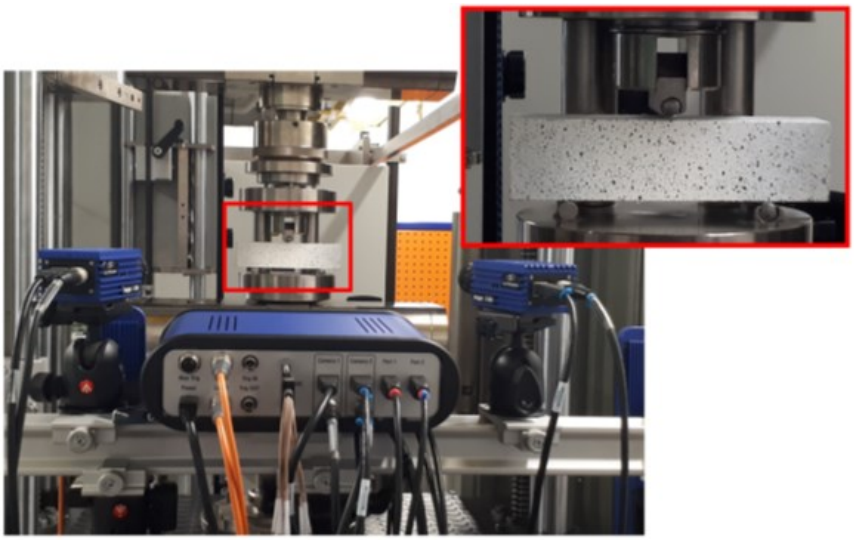

Figure 2: The flexural strength testing apparatus

2.3 Drying shrinkage

The shrinkage of each fibre-reinforced sample is measured using a digital strain gauge. In figure 3, the device is shown during a measurement of one of the samples.

Figure 3: Shrinkage measurement test set up

The shrinkage is measured at least three times a week until the length change becomes constant. The shrinkage is measured by comparing the current length of the sample with

the initial length, which was measured right after demoulding. The change of length on the shrinkage graph is calculated with Equation 3.

$$\Delta l = \frac{l_n - l_0}{l_0} \quad (3)$$

Where the initial length of the sample is denoted as l_0, and the nth measurement as l_n.

2.4 Freeze/thaw test

Freeze-thaw resistance was tested according to ASTM C 666/C 666M standard. The test was performed on prismatic beams (40 x 40 x 160 mm). The samples were placed in a tray and submerged 50 % in air and 50 % in water.

The freeze-thaw cycles were from +15°C to -15°C, with a period of 6h for a cycle. Samples were removed after 60 and 120 cycles, allowed to dry at 23°C and 35 % relative humidity for one day, and compressive strength and flexural strength will be measured.

3 RESULTS AND DISCUSSION

3.1 Compressive Strength

Equation 1 was used to calculate the strength. From the results presented in table 4, it can be clearly seen, that the total compressive strength decreases as the proportion of fly ash increases in the mix composition. However, after the 28-day measurements, it is evident that the relative increase of strength is higher when the fly ash content is higher.

Table 4: Compressive strength tests results after 7 and 28 days

Mix Composition	7 days compressive strength (MPa)	28 days compressive strength (MPa)
Reference	83,21	96,50
F1CW	81,38	90,33
F2CW	72,78	82,88
F3CW	49,19	65,73
F4CW	34,38	52,84

It is common knowledge in the field that fibre-reinforcement does not affect the compressive strength of a concrete specimen, so it is not calculated for the different fibre mixtures. In other words, it can be assumed that for all fibre-reinforced samples in the next section, the compressive strength stays constant.

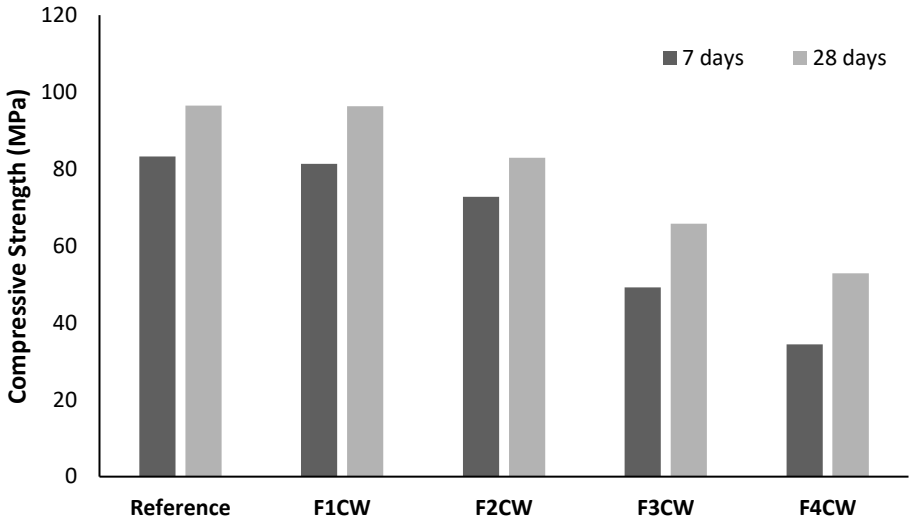

Figure 4: Compressive strength results for 7 and 28 days

3.2 Flexural Strength

Flexural strength was measured using the three-point bending test, and the results are calculated based on Equation 2. In Table 5, results of the flexural strength test after 28 days are shown for the different mix compositions, including the reference sample. The results indicate that after 7 days, F1CW is ≈ 9 % weaker than the reference, but after 28 days it is only ≈ 2,5 % weaker. After 7 days, F2CW is ≈ 10 % weaker than the reference, and after 28 days the difference is ≈ 7 % of the flexural load compared to the reference.

F3CW and F4CW are noticeably weaker in flexural strength. After 7 days, F3CW is 73 % weaker than reference, and F4CW is ≈ 57 %. After 28 days, F3CW is still ≈ 73 % of the strength of the reference specimen and F4CW has increased up to ≈ 70 % of the strength of the reference specimen.

Table 5: Flexural strength results

Mix Composition	7 days flexural strength (MPa)	28 days flexural strength (MPa)
Reference	7,15	8,33
F1CW	6,51	8,12
F2CW	6,46	7,72
F3CW	5,22	6,11
F4CW	4,06	5,79

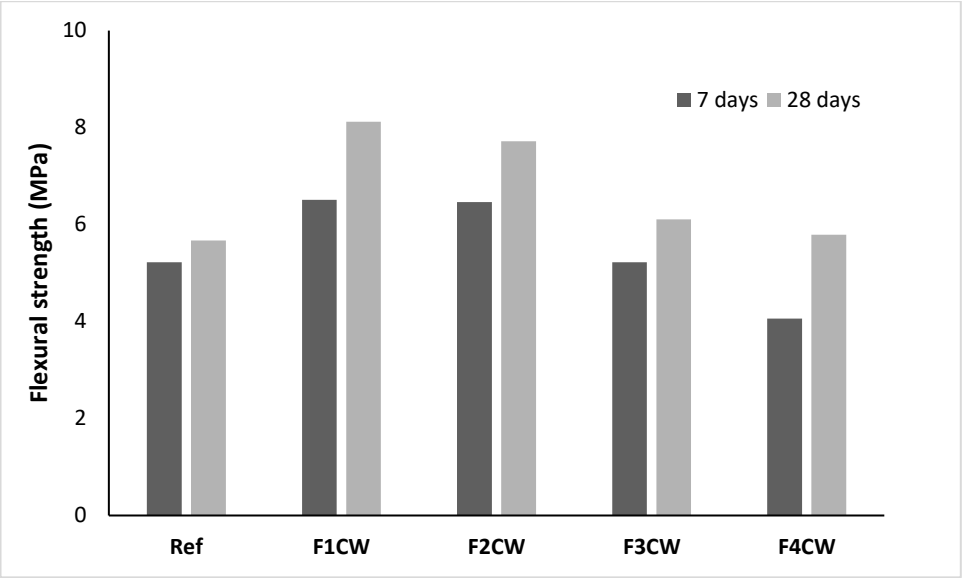

Figure 5: Flexural strength results after 28 days

Table 6: Flexural strength test results after 28 days

Mixtures	Flexural strength (MPa)
Reference (F3CW)	6,11
a) 1,5 Basalt	11,02
b) 1,5 PP	7,84
c) 0,75 Ba 0,75 PP	9,44
d) 1,0 Ba 0,5 PP	9,25
e) 0,5 Ba 1,0 PP	9,32
f) 0,5 PVA 1,0 PP	7,96
g) 0,75 PVA 0,75 Basalt	10,93
h) 0,5 PVA 1,0 Basalt	10,38
i) 1,5 PVA	10,75
j) 0,75 PVA 0,75 PP	10,13
k) 1,0 PVA 0,5 Ba	10,52
l) 1,0 PVA 0,5 PP	9,41

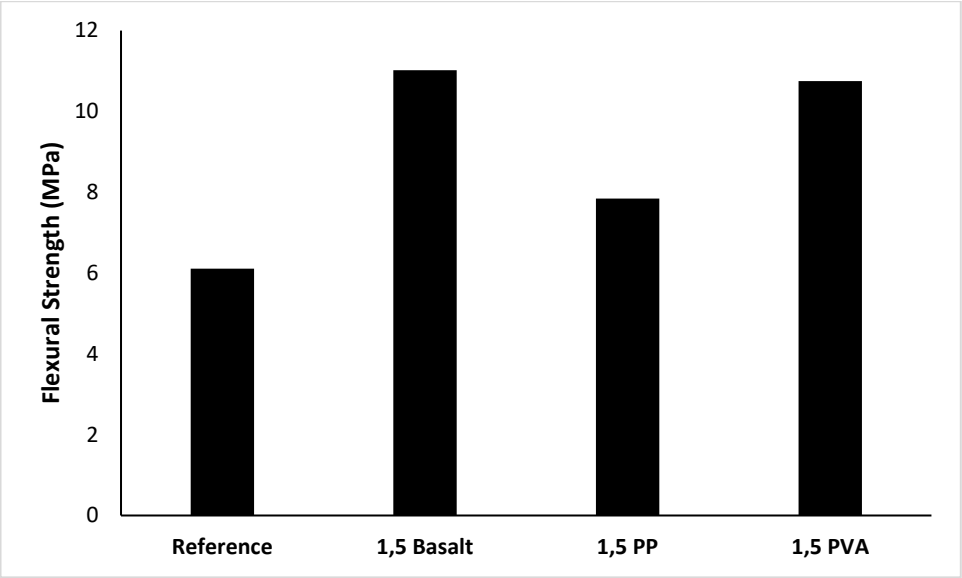

Figure 6: The flexural strength of samples a, b, i compared to reference.

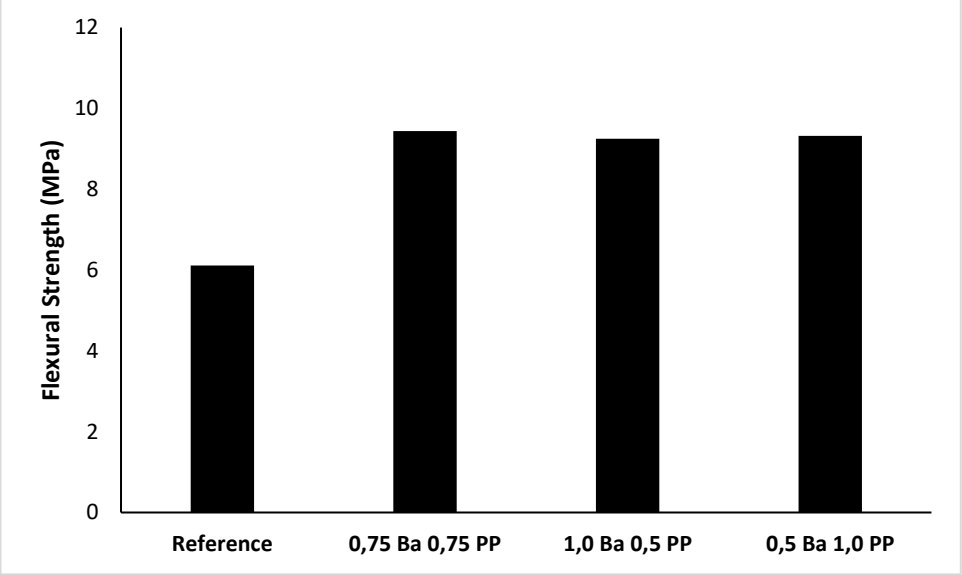

Figure 7: The flexural strength of samples c, d, e compared to reference.

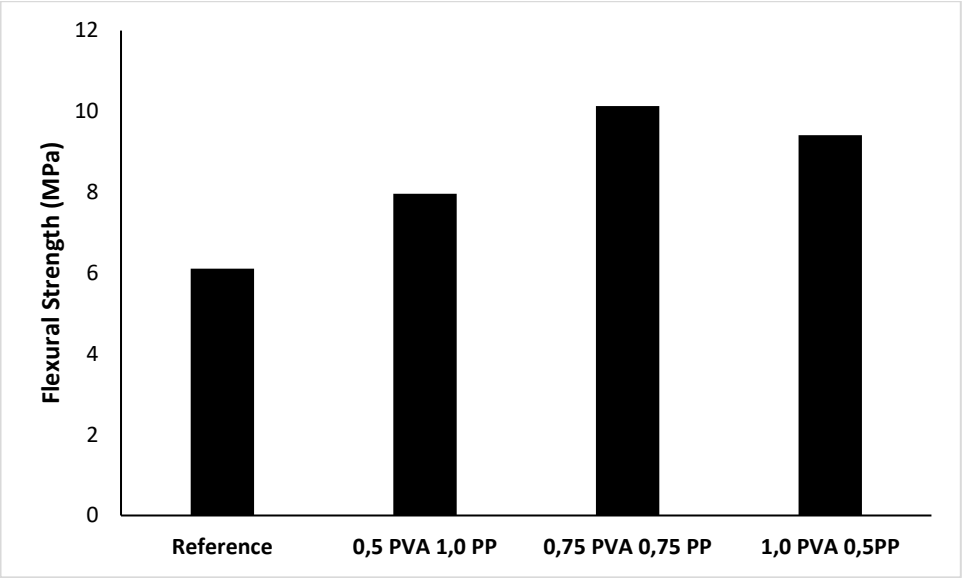

Figure 8: The flexural strength of samples f, j, l compared to reference.

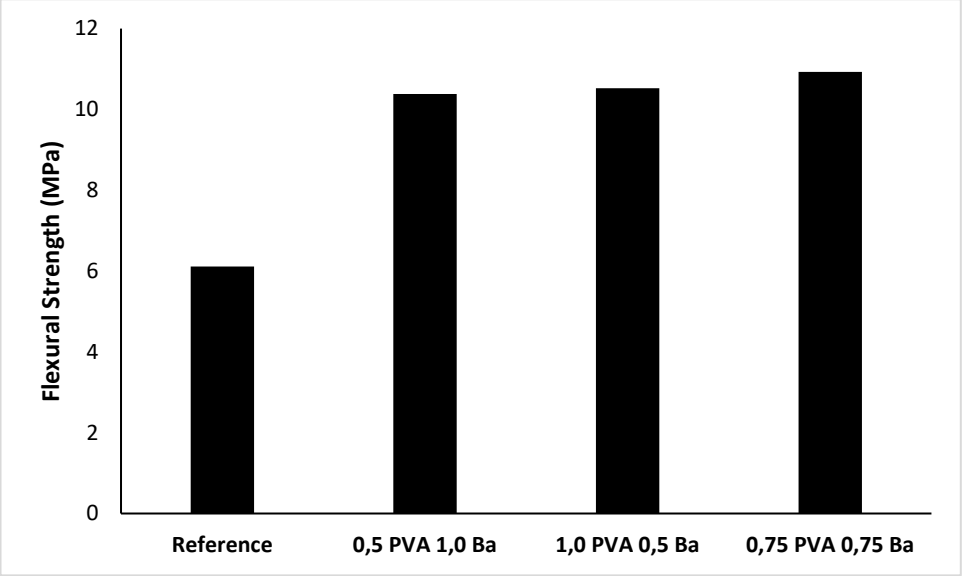

Figure 9: The flexural strength of samples g, h, k compared to reference.

3.3 Drying shrinkage

The drying shrinkage of the fibre-reinforced samples was measured and the length change was calculated using Equation 3. In Figures 10-13, the changes of length compared to the initial length are displayed as a function of time. The results are completely governed by the fibre combinations.

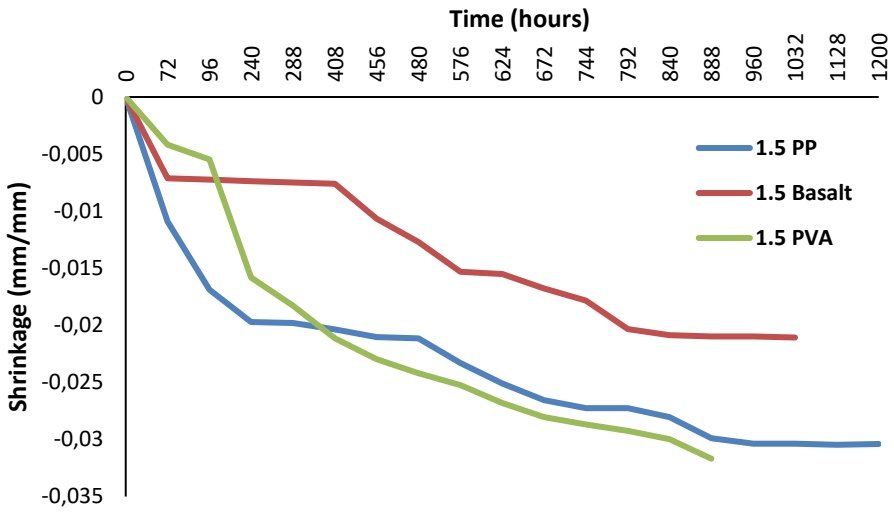

Figure 10: Drying shrinkage of the mix compositions with PP, PVA, Basalt fibres

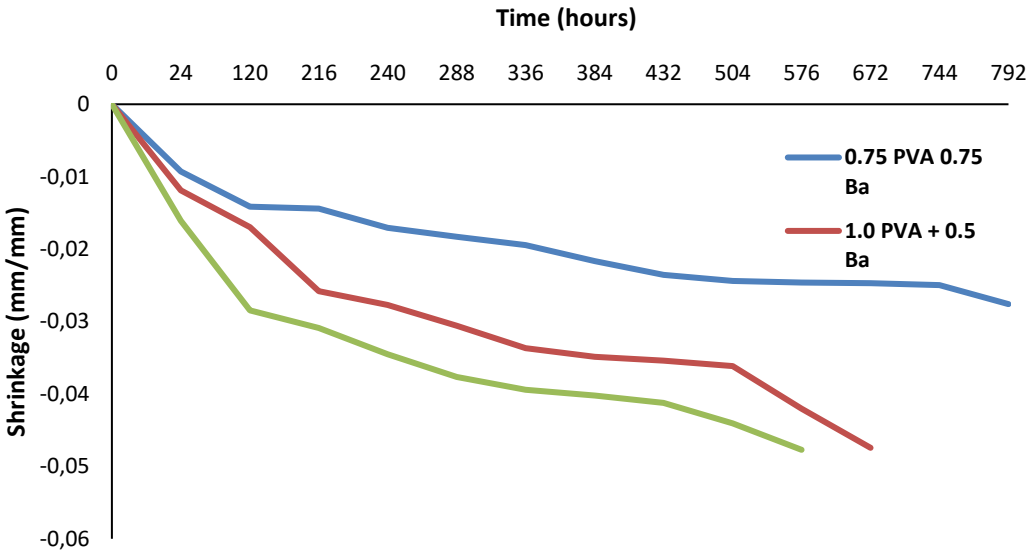

Figure 11: Shrinkage of PVA and Basalt mixes.

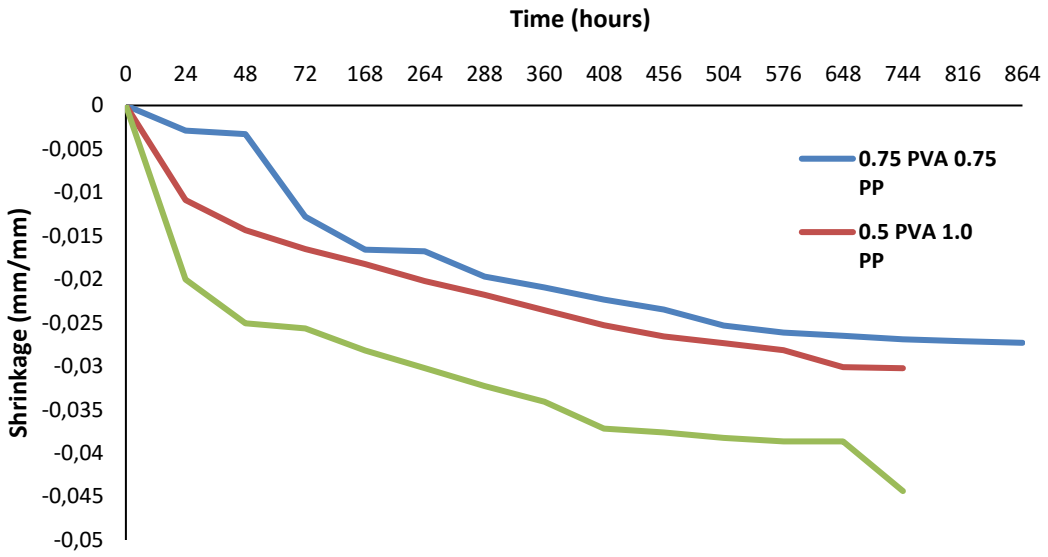

Figure 12: Shrinkage of PVA and PP mixes.

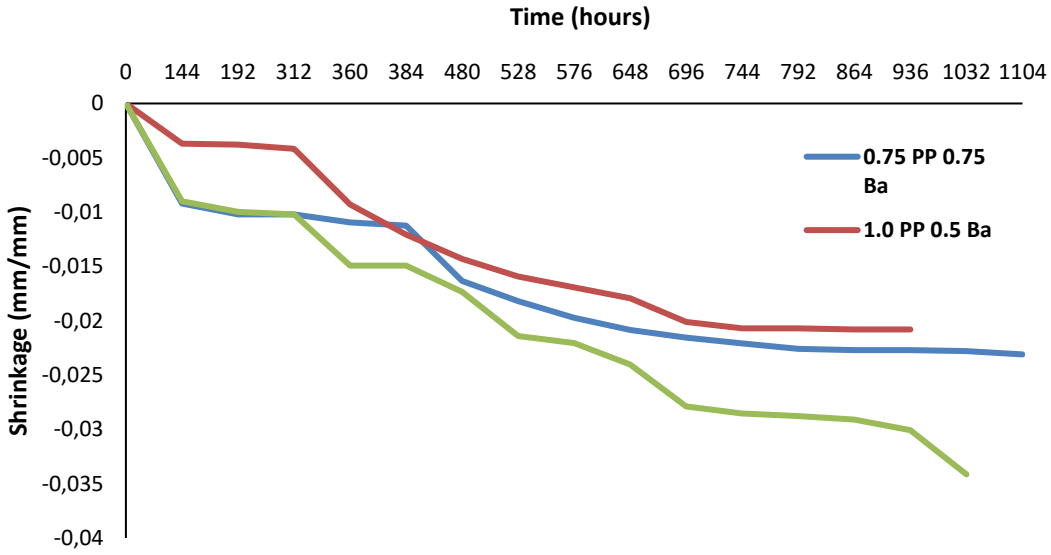

Figure 13: Shrinkage of PP and Basalt mixes.

3.4 Freeze/thaw results

Compressive strength tests were performed on the samples that underwent the freeze-thaw test. In Figures 14-17 the results are shown and compared to the reference specimen's strength. As seen from the figures, some mixes, like PP + Ba and PP + PVA perform approximately equally compared to the reference, while some other mixes like 1,0 PVA 0,5 Ba and 1,0 PVA 0,5 PP perform weaker.

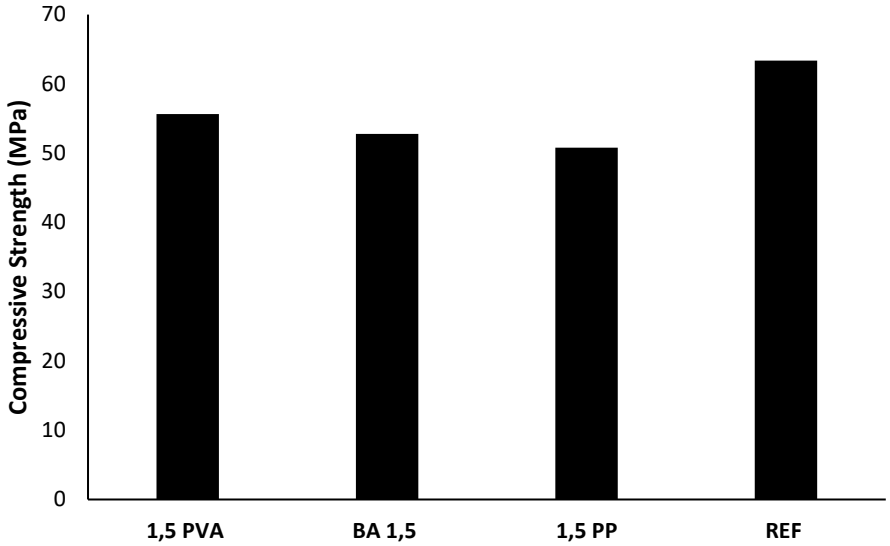

Figure 14: Compressive strength after freeze-thaw cycles.

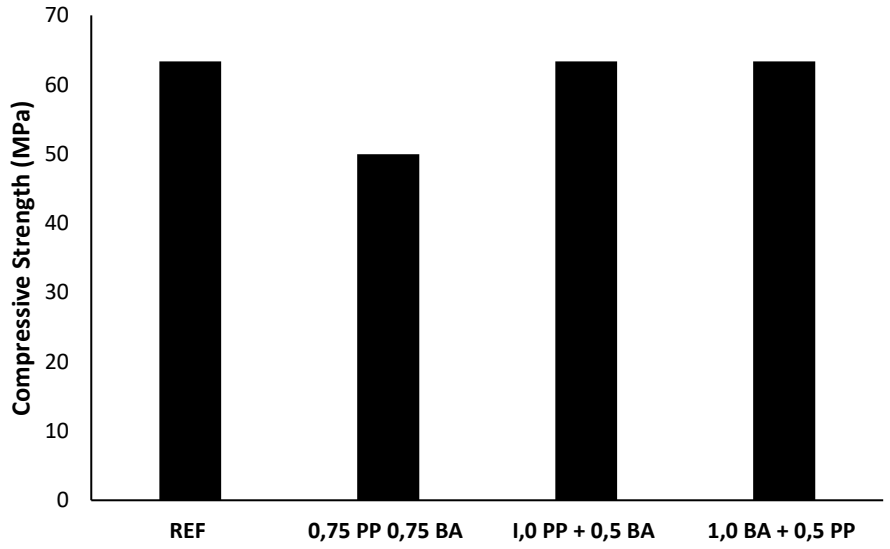

Figure 15: Compressive strength of PP + Ba mixes after freeze-thaw cycles.

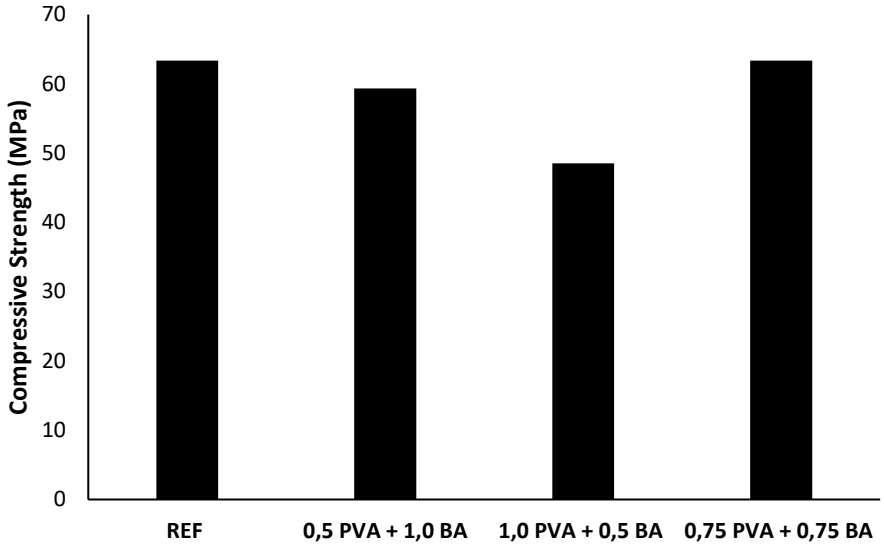

Figure 16: Compressive strength of PVA + Ba mixes after freeze-thaw cycles.

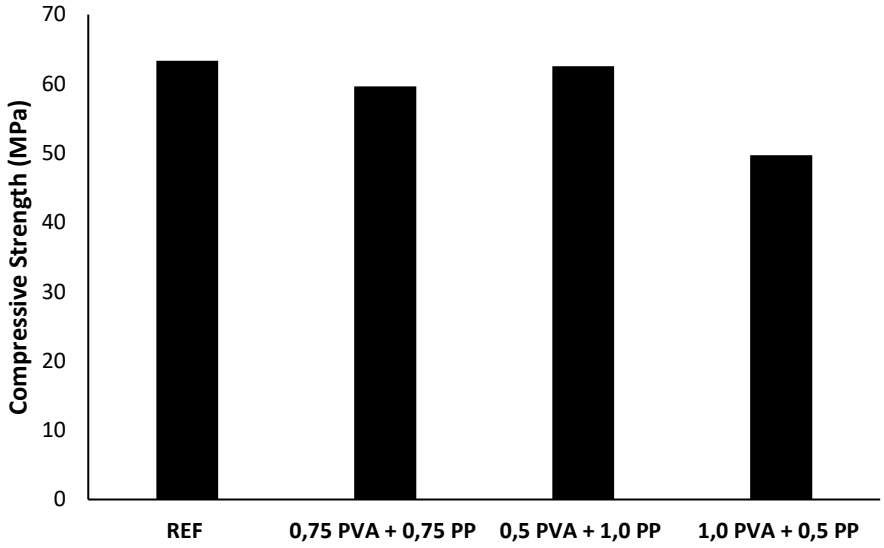

Figure 17: Compressive strength of PVA + PP mixes after freeze-thaw cycles.

In Table 7, the flexural strength test results after the freeze test are listed in Figures 18-21. From the graphs the effect of freeze-thaw cycles can be seen clearly. Some fibre combinations, like PVA + Basalt, seem to have good resistance against freeze-thaw effects. According to the results, polypropylene fibre appears to have the weakest performance in low temperature condition.

Table 7: Flexural strength after freeze-test.

Sample	Flexural Strength (MPa)
Reference (F3CW)	7,36
1,5 Ba	9,07
1,5 PP	6,03
1,5 PVA	10,22
F2CW Ref	7,36
0,75 Ba 0,75 PP	5,2
1,0 Ba 0,5 PP	8,26
0,5 Ba 1,0 PP	5,76
0,5 PVA 1,0 PP	7,88
0,75 PVA 0,75 PP	7,48
1,0 PVA 0,5PP	6,88
0,75 PVA 0,75 Ba	10,2
0,5 PVA 1,0 Ba	8,96
1,0 PVA 0,5 Ba	8,14

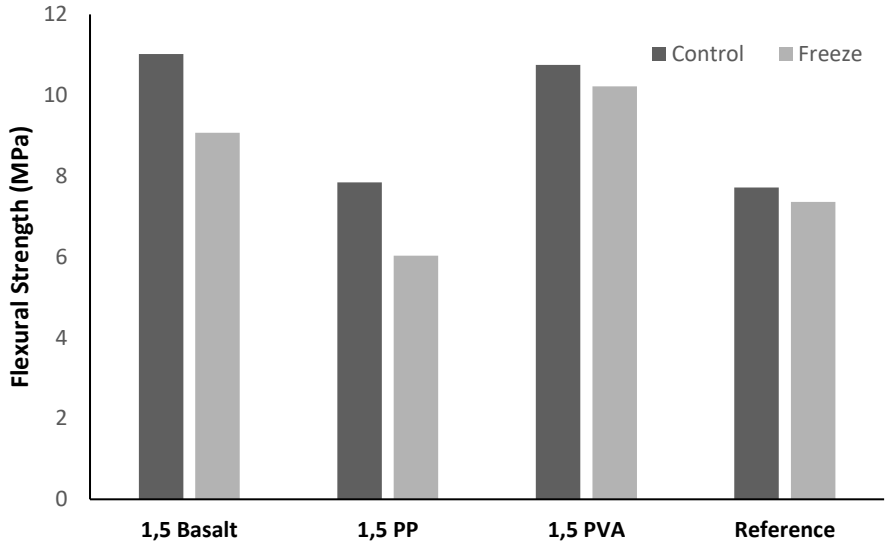

Figure 18: Comparing freeze-tested strength to original specimens.

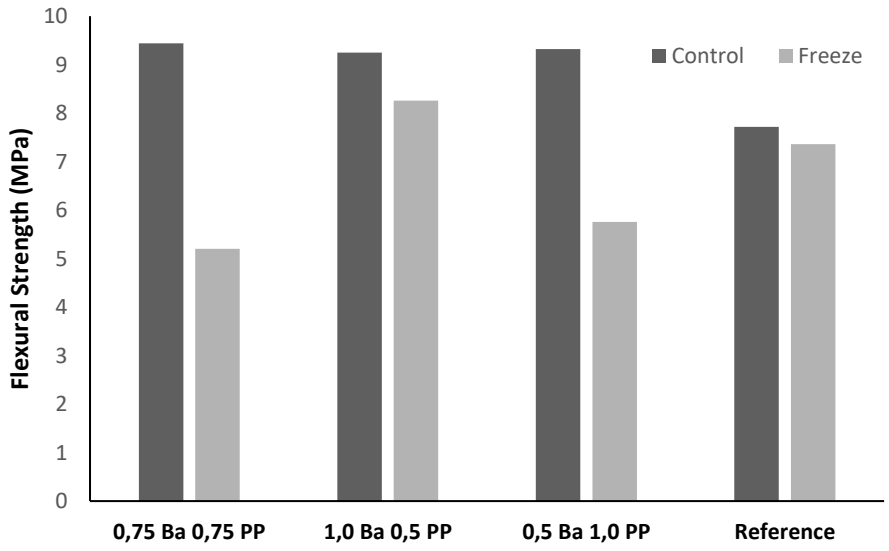

Figure 19.

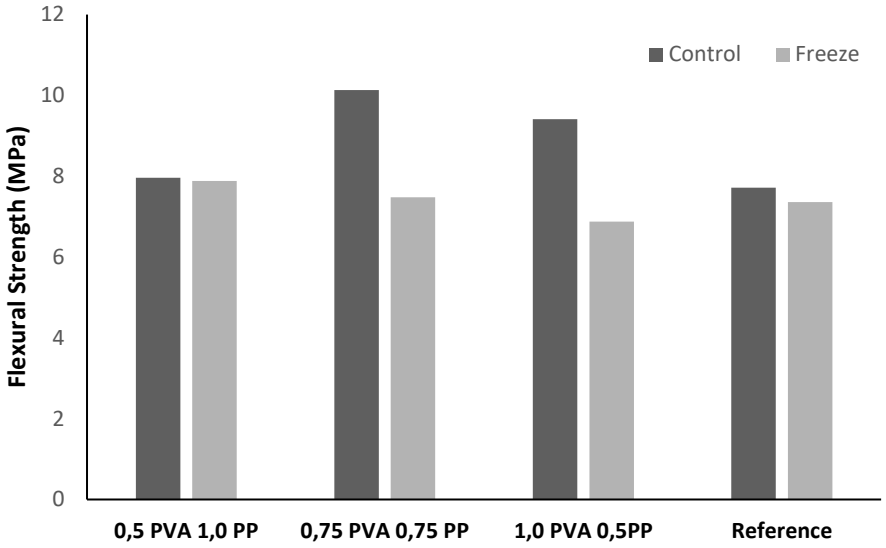

Figure 20.

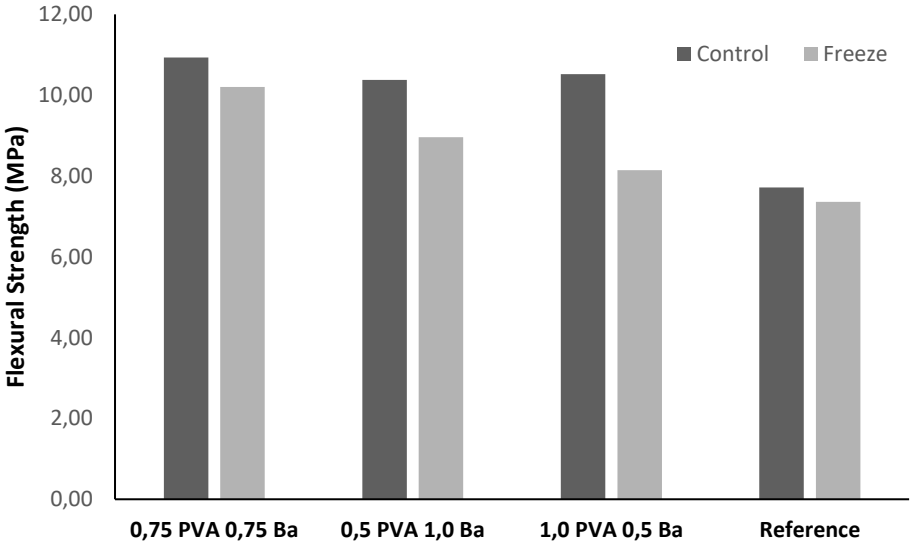

Figure 21.

4 CONCLUSION

In this study, the properties of alkali-activated binders with crushed ceramic aggregate was investigated. The effect of replacing slag by fly ash up to 80% of the total binder has been investigated based on the mechanical strength results. Then, different fibre combinations were used to improve mechanical strengths and minimize the negative effects of the drying shrinkage. Regarding the results obtained, the following conclusions could be highlighted:

Firstly, regardless of the curing time, fly ash as a replacement of blast furnace slag reduced the compressive strength. The reduction was proportional to the amount of fly ash replacing the slag. This reduction was also validated for the flexural strength. An interesting detail revealed, was that increasing the fly ash content above 50 % had no great impact on the flexural strength.

Secondly, adding fibres improved the flexural strength of the specimens, so that the maximum increase in performance was measured at more than 40 % in the reinforced mixtures with only 1.5 % basalt fibre as mono-fibre or 0.75 PVA+0.75 Basalt fibres as hybrid fibres. This enhancement could be justified by fibre bridging action.

In addition, after performing the freeze and thaw test, it was observed that the strength loss was governed by the fibre combination. Concerning the results, the lowest flexural strength loss was recorded about 5% in the mixtures incorporating 1.5%PVA fibres, while the minimum strength loss for hybrid fibres was recorded 7% for 0.75 PVA+0.75 Basalt fibres.

Lastly, promising results were obtained in controlling the drying shrinkage due to use of hybrid fibres, as compared to single fibre type. The results confirmed that the fibre combination could reduce the rate of drying shrinkage even lower than 0.02.

5 REFERENCES

Abdollahnejad, Z., Mastali, M., Luukkonen, T., Kinnunen, P., Illikainen, M., 2018. Fiber-reinforced one-part alkali-activated slag/ceramic binders. Ceramics International.

Akbarnezhad, A., Huan, M., Mesgari, S., Castel, A., 2015. Recycling of geopolymer concrete. Construction and building materials, Vol 101. pp. 152 – 158.

Amin, Sh. K., Sibak, H. A., El-Sherbiny, S. A., Abadir, M. F., 2016. An Overview of Ceramic Wastes Management in Construction. International Journal of Applied Engineering Research, Vol 11(4).

Ariffin, M. A., Hussin, M. W., Samadi, M., Lim, N. H., Mirza, J., Awalludin, D., Othman, N., 2015. Effect of Ceramic Aggregate on High Strength Multi Blended Ash Geopolymer Mortar. Jurnal Teknologi, Vol 77(16). pp. 33 – 36.

ASTM C666 / C666M-15, 2015. Standard Test Method for Resistance of Concrete to Rapid Freezing and Thawing, ASTM International, West Conshohocken, PA.

Bernal, S. A., Provis, J. L., San Nicholas, R., van Deventer, J. S. J., 2015. Alkali-activated slag cements produced with a blended sodium carbonate/sodium silicate activator. Advances in Cement Research, Vol 28(4). pp. 262-273.

Davidovits, J., 1994. Global warming impact on the cement and aggregates industries. World research review, Vol 6(2). pp. 263-278.

Davidovits, J., 2008. Geopolymer chemistry and applications. 2nd edition. Saint Quentin, France: Institut Géopolymère. ISBN: 978-295-14-8201-2

Fernández-Jiménez, A., Palomo, A., 2005. Composition and microstructure of alkali activated fly ash binder: Effect of the activator. Cement and Concrete Research, Vol 35(10). pp. 1984-1992.

Gao, X., 2017. Alkali activated slag-fly ash binders: design, modelling and application. Department of Built Environment, Technische Universiteit Eindhoven.

Halicka, A., Ogrodnik, P., Zegardlo, B., 2013. Using ceramic sanitary ware waste as concrete aggregate. Construction and Building Materials, Vol 48. pp. 295-305.

Kiisa, M., Lellep, K., Trossek, M., 2016. The effect of basalt fibre on the properties of normal-weight concrete. Professional Studies: Theory and Practice, Vol 1(16). P. 51 – 63.

Luukkonen, T., Abdollahnejad, Z., Yliniemi, J., Kinnunen, P., Illikainen, M., 2018. One-part alkali-activated materials: A review. Cement and Concrete Research, Vol 103. pp. 21-34.

Manfaluthy, M. L., Ekaputri J. J., 2017. The Application of PVA Fiber to Improve the Mechanical Properties of Geopolymer Concrete. MATEC Web of Conferences, Vol 138. Article number: 01020.

Pacheco-Torgal, F., Jalali, S., 2010. Compressive strength and durability properties of ceramic wastes based concrete. Materials and Structures Vol 44. P. 155-167.

Pilehvar, S., Pamies, R., Lanzón, M., Valentini, L., Carmona, M., Szczotok, A. M., Cao, V. D., Kjøniksen, A.-L., 2018. Physical and mechanical properties of fly ash and slag geopolymer concrete containing different types of micro-encapsulated phase change materials. Construction and Building Materials Vol 173. pp. 28-39.

Provis J. L., Van Deventer J. S. J., 2014. Alkali-Activated Materials State-of-the-Art Report, RILEM TC 224-AAM.

Sankar, K., Stynoski, P., Al-Chaar, G. K., Kriven W. M., 2017. Sodium silicate activated slag-fly ash binders: Part I – Processing, microstructure, and mechanical properties. Journal of American Ceramic Society, Vol 101(6).

Seymour, P., 2010. The eco-friendly durable low-energy alternative to OPC. Construct Ireland, Vol 2(12).

Srinivasreddy K., Srinivasan, K., 2017. Review on supplementary cementitious materials used in inorganic polymer concrete. IOP Conference Series: Materials Science and Engineering, Vol 263. Article number: 032023.

Zhu, J., Zheng, W. Z., Qin, C. Z., Xu, Z. Z., Wu, Y. Q., 2018. Effect of different fibres on mechanical properties and ductility of alkali-activated slag cementitious material. IOP Conference Series: Materials Science and Engineering, Vol 292.